

# The dynamics of starvation and recovery

<sup>1</sup> Justin D. Yeakel \* †‡, Christopher P. Kempes †, and Sidney Redner †§

<sup>3</sup> \*School of Natural Science, University of California Merced, Merced, CA, †The Santa Fe Institute, Santa Fe, NM, §Department of Physics, Boston University, Boston  
<sup>4</sup> MA, and ‡To whom correspondence should be addressed: jdyeakel@gmail.com

<sup>5</sup> Submitted to Proceedings of the National Academy of Sciences of the United States of America

**This is the abstract. [No it isn't. It's merely a placeholder.]**

foraging | starvation | reproduction

## Introduction

The behavioral ecology of most, if not all, organisms is influenced by the energetic state of individuals, which directly influences how they invest reserves in uncertain environments. Such behaviors are generally manifested as trade-offs between investing in somatic maintenance and growth, or allocating energy towards reproduction [1, 2, 3]. The timing of these behaviors responds to selective pressure, as the choice of the investment impacts future fitness [4]. The influence of resource limitation on an organism's ability to maintain its nutritional stores may lead to repeated delays or shifts in reproduction over the course of an organism's life.

The life history of most species is typically comprised of (a) somatic growth and maintenance, and (b) reproduction. The balance between these two activities is often conditioned on resource availability [5]. For example, reindeer invest less in calves born after harsh winters (when the mother's energetic state is depleted) than in calves born after moderate winters [6]. Many bird species invest differently in broods during periods of resource scarcity compared to normal periods [7, 8], sometimes delaying or even foregoing reproduction for a breeding season [1, 9, 10]. Even freshwater and marine zooplankton have been observed to avoid reproduction under nutritional stress [11], and those that do reproduce have lower survival rates [2]. Organisms may also separate maintenance and growth from reproduction over space and time: many salmonids, birds, and some mammals return to migratory breeding grounds to reproduce after one or multiple seasons in resource-rich environments where they accumulate nutritional reserves [12, 13, 14].

Physiological mechanisms also play an important role in regulating reproductive expenditures during periods of resource limitation. The data collected thus far has shown that diverse mammals (47 species in 10 families) exhibit delayed implantation, whereby females postpone fetal development (blastocyst implantation) until times where nutritional reserves can be accumulated [15, 16]. Many other many species (including humans) suffer irregular menstrual cycling and higher spontaneous abortion rates during periods of nutritional stress [17, 18]. In the extreme case of unicellular organisms, nutrition is unavoidably linked to reproduction because the nutritional state of the cell regulates all aspects of the cell cycle [19]. The existence of so many independently evolved mechanisms across such a diverse suite of organisms highlights the importance and universality of the fundamental tradeoff between somatic and reproductive investment. However the dynamic implications of these constraints are unknown.

Though straightforward conceptually, incorporating the energetic dynamics of individuals [20] into a population-level framework [20, 21] presents numerous mathematical obstacles [22]. An alternative approach involves modeling the macroscale relations that guide somatic versus reproductive investment in a consumer-resource system. For example, macroscale Lotka-Volterra models assume that the growth rate of the consumer population depends on resource density, thus

implicitly incorporating the requirement of resource availability for reproduction [23].

In this work, we adopt an alternative approach in which resource limitation and the subsequent effect of starvation is accounted for explicitly. Namely, only individuals with sufficient energetic reserves can reproduce. Such a constraint leads to reproductive time lags due to some members of the population going hungry and then recovering. Additionally, we incorporate the idea that reproduction is strongly constrained allometrically [3], and is not generally linearly related to resource density. As we shall show, these constraints influence the ensuing population dynamics in dramatic ways.

## Nutritional-state-structured model (NSM)

We begin by defining a minimal Nutritional-State-structured population Model (NSM), where the consumer population is divided into two energetic states: (a) an energetically replete (full) state  $F$ , where the consumer reproduces at a constant rate  $\lambda$  and has no mortality risk, and (b) an energetically deficient (hungry) state  $H$ , where the consumer does not reproduce but dies at rate  $\mu$ . The underlying resource  $R$  evolves by logistic growth with an intrinsic growth rate  $\alpha$  and a carrying capacity equal to one. Consumers transition from the full state  $F$  to the hungry state  $H$  by starvation at rate  $\sigma$  and also in proportion to the absence of resources  $(1 - R)$ . Conversely, consumers recover from state  $H$  to state  $F$  at rate  $\rho$  and in proportion to  $R$ . Resources are also eaten by the consumers—at rate  $\rho$  by hungry consumers and at rate  $\beta < \rho$  by full consumers. This inequality accounts for hungry consumers requiring more resources to rebuild body weight.

In the mean-field approximation, in which the consumers and resources are perfectly mixed, their densities evolve according to the rate equations

$$\begin{aligned}\dot{F} &= \lambda F + \rho RH - \sigma(1 - R)F, \\ \dot{H} &= \sigma(1 - R)F - \rho RH - \mu H, \\ \dot{R} &= \alpha R(1 - R) - R(\rho H + \beta F).\end{aligned}\quad [1]$$

Notice that the total consumer density  $F + H$  evolves according to  $\dot{F} + \dot{H} = \lambda F - \mu H$ . This resembles the equation of motion for the predator density in the classic Lotka-Volterra model, except that the resource density does not appear in the growth term. As discussed above, the attributes of reproduction and mortality have been explicitly apportioned to the full and hungry consumers, respectively, so that the growth in the total density is decoupled from the resource density.

## Reserved for Publication Footnotes

103 Equation [1] has three fixed points: two trivial fixed points 161 If  $\rho$  exceeds a threshold value, cyclic dynamics will develop as  
 104 at  $(F^*, H^*, R^*) = (0, 0, 0)$  and  $(0, 0, 1)$ , and one non-trivial, 162 the Hopf bifurcation is approached.  
 105 internal fixed point at

$$F^* = \frac{\alpha\lambda\mu(\mu + \rho)}{(\lambda\rho + \mu\sigma)(\lambda\rho + \mu\beta)},$$

$$H^* = \frac{\alpha\lambda^2(\mu + \rho)}{(\lambda\rho + \mu\sigma)(\lambda\rho + \mu\beta)},$$

$$R^* = \frac{\mu(\sigma - \lambda)}{\lambda\rho + \mu\sigma}.$$

106 The stability of this fixed point is determined by the Jaco- 161  
 107 bian Matrix  $\mathbf{J}$ , where each matrix element  $J_{ij}$  equals  $\partial\dot{X}_i/\partial X_j$   
 108 when evaluated at the internal fixed point, and  $\mathbf{X}$  is the vec- 162  
 109 tor  $(F, H, R)$ . The parameters in Eq. [1] are such that the 163  
 110 real part of the largest eigenvalue of  $\mathbf{J}$  is negative, so that the 164  
 111 system is stable with respect to small perturbations from the 165  
 112 fixed point. Because this fixed point is unique, it is the global 166  
 113 attractor for all population trajectories for any initial condition 167  
 114 where the resource and consumer densities are both non zero. 168

115 From Eq. [2], an obvious constraint on the NSM is that 169  
 116 the reproduction rate  $\lambda$  must be less than the starvation rate 170  
 117  $\sigma$ , so that  $R^*$  is positive. In fact, when the resource density 171  
 118  $R = 0$ , the rate equation for  $F$  gives exponential growth of 172  
 119  $F$  for  $\lambda > \sigma$ . The condition  $\sigma = \lambda$  represents a transcritical 173  
 120 (TC) bifurcation that demarcates the physical and unphysical 174  
 121 regimes [give Ref]. The biological implication of the constraint 175  
 122  $\lambda < \sigma$  has a simple interpretation—the rate at which a macro- 176  
 123 scopic organism loses mass due to lack of resources is generally 177  
 124 much faster than the rate of reproduction. As we will discuss 178  
 125 below, this inequality is a natural consequence of allometric 179  
 126 constraints [3] for organisms within empirically observed body 180  
 127 size ranges (Fig. 2).

128 In the physical regime of  $\lambda < \sigma$ , the fixed point [2] may 181  
 129 either be a stable node or a limit cycle (Fig. 3). In continuous- 182  
 130 time systems, a limit cycle arises when a pair of complex con- 183  
 131 jugate eigenvalues crosses the imaginary axis to attain positive 184  
 132 real parts [24]. This Hopf bifurcation is defined by  $\text{Det}(\mathbf{S}) = 0$ , 185  
 133 with  $\mathbf{S}$  the Sylvester matrix, which is composed of the coef- 186  
 134 ficients of the characteristic polynomial of the Jacobian ma- 187  
 135 trix [25]. As the system parameters are tuned to be within the 188  
 136 stable regime but close to the Hopf bifurcation, the amplitude of 189  
 137 the transient but decaying cycles become large. Given that eco- 190  
 138 logical systems are constantly being perturbed [26], the onset of 191  
 139 transient cycles, even though they decay with time in the mean- 192  
 140 field description, can increase the extinction risk [27, 28, 29]. 193  
 141 Thus the distance of a system from the Hopf bifurcation pro- 194  
 142 vides a measure of its persistence.

143 When the starvation rate  $\sigma \gg \lambda$ , a substantial fraction 195  
 144 of the consumers are driven to the hungry non-reproducing 196  
 145 state. Because reproduction is inhibited, there is a low steady- 197  
 146 state consumer density and a high steady-state resource den- 198  
 147 sity. However, if  $\sigma/\lambda \rightarrow 1$  from above, the population is 199  
 148 overloaded with energetically-replete (reproducing) individuals, 200  
 149 thereby promoting oscillations between the consumer and re- 201  
 150 source densities (Fig. 3).

151 Whereas the relation between consumer growth rate  $\lambda$  and 202  
 152 the starvation rate  $\sigma$  defines an absolute bound of biological 203  
 153 feasibility—the TC bifurcation—the starvation rate  $\sigma$  also de- 204  
 154 termines the sensitivity of the consumer population to changes 205  
 155 in resource density. When  $\sigma \gg \lambda$ , the steady-state population 206  
 156 density is small, thereby increasing the risk of stochastic ex- 207  
 157 tinction. On the other hand, as  $\sigma$  decreases, the system will 208  
 158 ultimately be poised either near the TC or the Hopf bifurcation 209  
 159 (Fig. 3). If the recovery rate  $\rho$  is sufficiently small, the TC bi- 210  
 160 furcation is reached and the resource eventually is eliminated. 211

163 [mention and refer to the starving random walk  
 164 model somewhere.]

165  
 166 **Role of allometry**  
 167 The NSM describes a broad range of dynamics, yet organisms 168  
 168 are likely unable to access most of the total parameter space. 169  
 169 Here we use allometric scaling relations to constrain the covaria- 170  
 170 tion of rates in a principled and biologically meaningful manner. 171  
 171 Allometric scaling relations highlight common constraints and 172  
 172 average trends across large ranges in body size and species di- 173  
 173 versity. Many of these relations can be derived from a small set 174  
 174 of assumptions and below we describe a framework to deter- 175  
 175 mine the covariation of timescales and rates across the range of 176  
 176 mammals for each of the key parameters of our model (cf. [30]). 177  
 177 We are thereby able to define the regime of dynamics occupied 178  
 178 by the entire class of mammals along with the key differences 179  
 179 between the largest and smallest mammals.

180 Nearly all of the rates described in the NSM are to some 181 extent governed by consumer metabolism, which can be used to 182 describe a variety of organismal features [Ref]. The scaling 183 relation between an organism's metabolic rate  $B$  and its body 184 size at reproductive maturity  $M$  is well documented [31] and 185 scales as  $B = B_0 M^\eta$ , where  $\eta$  is the scaling exponent, gener- 186 ally assumed to vary around 2/3 or 3/4 for metazoans [Ref], 187 and has taxonomic shifts for unicellular species between  $\eta \approx 1$  188 in eukaryotes and  $\eta \approx 1.76$  in bacteria [32, 3]. Several efforts 189 have shown how a partitioning of this metabolic rate between 190 growth and maintenance purposes can be used to derive a gen- 191 eral equation for the growth trajectories and growth rates of 192 organisms ranging from bacteria to metazoans [3, ?][fix Ref]. 193 More specifically, the interspecific [what does interspecific 194 mean?] trends in growth rate can be approximated by

$$\lambda = \lambda_0 M^{\eta-1}. \quad [3]$$

195 This relation is derived from the simple balance condition

$$B_0 m^\eta = E_m \frac{dm}{dt} + B_m m, \quad [4]$$

196 where  $E_m$  is the energy needed to synthesize a unit of mass, 197  $B_m$  is the metabolic rate to support an existing unit of mass, 198 and  $m$  is the mass at any point in development. It is useful to 199 explicitly write this balance because it can also be modified to 200 understand the timescales of both starvation and recovery from 201 starvation as we show below.

202 To determine the starvation rate,  $\sigma$ , we are interested in 203 the time required for an organism to go from a mature adult 204 that reproduces at rate  $\lambda$  (henceforth we term this state as the 205 "replete" state), to a reduced-size hungry state where reproduc- 206 tion is impossible. This transition time can be inferred from the 207 energy balance in Eq. 4, where we make the basic assumption 208 that an organism must meet its maintenance requirements us- 209 ing the digestion of existing mass as the sole energy source. 210 This assumption implies the simple metabolic balance [don't 211 understand this equation]

$$\frac{dm}{dt} E'_m = -B_m m \quad [5]$$

212 where  $E'_m$  is the amount of energy stored in a unit of existing 213 body mass which differs from  $E_m$  [Ref], the energy required 214 to synthesis a unit of biomass. Given the replete mass,  $M$ , 215 of an organism, the above energy balance prescribes the mass 216 trajectory of a non-consuming organism:

217 Since only certain tissues can be digested for energy (for ex- 218 ample the brain cannot be degraded to fuel metabolism), we 219

219 define the rate for starvation and death by the timescales re- 271 bifurcation increases, while uncertainty in allometric param-  
 220 quired to reach specific fractions of the replete-state mass. We 272 ters (20% variation around the mean; Fig. 4) results in little  
 221 define  $m_{\text{starve}} = \epsilon M$ , where  $\epsilon < 1$  is the fraction of replete-state 273 qualitative difference in the distance to the Hopf bifurca-  
 222 mass where reproduction ceases. This fraction will be modified 274 tion. These results suggest that small mammals are more prone  
 223 if tissue composition systematically scales with adult mass. For 275 to population oscillations—including both stable limit cycles as  
 224 example, making use of the observation that body fat in mam- 276 well as transient cycles—than mammals with larger body size.  
 225 mals scales with overall body size according to  $M_f = f_0 M^\gamma$  277 Thus our NSM model predicts that population cycles should be  
 226 and assuming that once this mass is fully digested the organism 278 less common for larger species and more common for smaller  
 227 begins to starve, this would imply that  $\epsilon = 1 - f_0 M^\gamma / M$ . Using 279 species, particularly in environments where resources are limit-  
 228 this criterion in Eq. 6, the time scale for starvation is given by 280 ing.

$$t_\sigma = -\frac{E_m \ln(\epsilon)}{B_m}.$$

229 The starvation rate is then  $\sigma = 1/t_\sigma$ , which scales with replete- 281 bifurcation increases, while uncertainty in allometric param-  
 230 state mass as  $1/\ln(1 - f_0 M^\gamma / M)$ . An important feature is 282 ters (20% variation around the mean; Fig. 4) results in little  
 231 that  $\sigma$  does not have a simple scaling dependence on  $\lambda$  (Eq. 3), 283 qualitative difference in the distance to the the Hopf bifurca-  
 232 which is important for the dynamics that we later discuss. 284 tion. These results suggest that small mammals are more prone  
 233 The time to death should follow a similar relation, but de- 285 if tissue composition systematically scales with adult mass. For  
 234 fined by a lower fraction of replete-state mass,  $m_{\text{death}} = \epsilon' M$ . 286 example, making use of the observation that body fat in mam-  
 235 Suppose, for example, that an organism dies once it has digested 287 mals scales with overall body size according to  $M_f = f_0 M^\gamma$ . 288 Thus our NSM model predicts that population cycles should be  
 236 all fat and muscle tissues, and that muscle tissue scales with 289 less common for larger species and more common for smaller  
 237 body mass according to  $M_{mm} = mm_0 M^\zeta$  [what is  $mm_0$ ?]. 290 species, particularly in environments where resources are limit-  
 238 This gives  $\epsilon' = 1 - (f_0 M^\gamma + mm_0 M^\zeta) / M$ . Muscle mass has 291 this criterion in Eq. 6, the time scale for starvation is given by 292 ing.

239 been shown to be roughly proportional to body mass [33] in 293 Previous studies have used allometric constraints to explain  
 240 mammals and thus  $\epsilon'$  is merely  $\epsilon$  minus a constant. Thus 294 the periodicity of cyclic populations [34, 35, 36], suggesting a pe-  
 295

$$t_\mu = -\frac{E_m \ln(\epsilon')}{B_m}$$

241 and  $\mu = 1/t_\mu$ .

242 The rate of recovery  $\rho = 1/t_\rho$  requires that an organism ac- 296 flux of the population to the hungry state. In this state repro-  
 243 crues sufficient tissue to transition from the starving [starving 297 duction is absent, thus increasing the likelihood of extinction.  
 244 vs. hungry] state to the full state. We again use the balance 298 However, from the perspective of population survival, it is the  
 245 given in Eq. 4 to find the timescale to return to the replete-state 299 rate of starvation relative to the rate of recovery that deter-  
 246 mass from a given reduced starvation mass. From the solution 300 mines the long-term dynamics of the system (Fig. 3). We now  
 247 to Eq. 4

$$m(t) = \left(\frac{B_0}{B_m}\right)^{1/(\eta-1)} \left[1 - \left(1 - \frac{B_m}{B_0} m_0^{1-\eta}\right) e^{-b(1-\eta)t}\right]^{1/(1-\eta)} \quad [9]$$

248 we require the timescale,  $t_\rho = t_2 - t_1$ , which is the time it takes 301 examine the competing effects of cyclic dynamics vs. changes in  
 249 to go from  $m(t_1) = \epsilon M$  to  $m(t_2) = M$ , or 302 steady state density on extinction risk as a function of the ratio  
 303  $\sigma/\rho$ . To this end, we computed the probability of extinction,  
 304 where extinction is defined as the population trajectory going  
 305 below  $0.2 \times$  the allometrically constrained steady state for all  
 306 times between  $10^2$  and  $\leq 10^6$ . This procedure is repeated for  
 307 1000 replicates of the continuous-time system shown in Eq. 1  
 308 for an organism of  $M = 100$  grams. In each replicate the initial  
 309 condition is distributed around the steady state (Eq. 2). Specif-  
 310 ically the initial densities are chosen to be  $A(F^*, H^*, R^*)$ , with  
 311  $A$  a random variable that is uniformly distribution in  $[0, 2]$ . By  
 312 allowing the rate of starvation to vary, we assessed extinction  
 313 risk across a range of values of the ratio  $\sigma/\rho$  varying between  
 314  $10^{-2}$  to  $2.5$ , thus examining a horizontal cross-section of Fig. 3.  
 315 As expected, higher rates of extinction correlated with both low  
 316 and high values of  $\sigma/\rho$ . For low values of  $\sigma/\rho$ , the increased  
 317 extinction risk results from transient cycles with larger ampli-  
 318 tudes as the system nears the Hopf bifurcation (Fig. 5). For  
 319 large values of  $\sigma/\rho$ , higher extinction risk arises because of to  
 320 the decrease in the steady state consumer population density.  
 321 This interplay creates an ‘extinction refuge’ as shown in Fig. 5,  
 322 such that for a relatively constrained range of  $\sigma/\rho$ , extinction  
 323 probabilities are minimized.

250 Although these rate equations are general, here we focus on pa- 324 We find that the allometrically constrained values of  $\sigma/\rho$   
 251 rameterizations for terrestrial-bound endotherms, specifically 325 (with  $\pm 20\%$  variability around energetic parameter means) fall  
 252 mammals, which range from a minimum of  $M \approx 1$  gram (the 326 within the extinction refuge. These values are close enough to  
 253 Etruscan shrew *Suncus etruscus*) to a maximum of  $M \approx 10^7$  327 the Hopf bifurcation to avoid low steady state densities, and  
 254 grams (the late Eocene to early Miocene Indricotheriinae). In- 328 far enough away to avoid large-amplitude transient cycles. The  
 255 vestigating other classes of organisms would simply involve al- 329 fact that allometric values of  $\sigma$  and  $\rho$  fall within this relatively  
 256 tering the metabolic exponents and scalings associate with  $\epsilon$ . 330 small window supports the possibility that a selective mech-  
 257 Moreover, we emphasize that our allometric equations describe 331 nism has constrained the physiological conditions that drive ob-  
 258 mean relationships, and do not account for the (sometimes con- 332 served starvation and recovery rates within populations. Such a  
 259 siderable) variance associated with individual species. 333 mechanism would select for organism physiology that generates  
 260

### 261 Stabilizing effects of allometric constraints

262 As the allometric derivations of the NSM rate laws reveal,  $\sigma$  and 334 appropriate  $\sigma$  and  $\rho$  values that avoid extinction. This selection  
 263  $\rho$  are not independent parameters, and the bifurcation space 335 could occur via the tuning of body fat percentages, metabolic  
 264 shown in Fig. 3 is navigated via covarying parameters. Given 336 rates, and biomass maintenance efficiencies. To summarize,  
 265 the parameters of terrestrial endotherms, we find that  $\sigma$  and  $\rho$  337 our finding that the allometrically-determined parameters fall  
 266 are constrained to lie within a small window of potential values  
 267 (Fig. 4) for the known range of body sizes  $M$ . We thus find that  
 268 the dynamics for all mammalian body sizes is confined to the  
 269 steady-state regime of the NSM and that limit-cycle behavior  
 270 is precluded. Moreover, for larger  $M$ , the distance to the Hopf

271 bifurcation increases, while uncertainty in allometric param-  
 272 ters (20% variation around the mean; Fig. 4) results in little  
 273 qualitative difference in the distance to the the Hopf bifurca-  
 274 tion. These results suggest that small mammals are more prone  
 275 to population oscillations—including both stable limit cycles as  
 276 well as transient cycles—than mammals with larger body size.  
 277 Thus our NSM model predicts that population cycles should be  
 278 less common for larger species and more common for smaller  
 279 species, particularly in environments where resources are limit-  
 280 ing.

### 294 Extinction risk

295 Within our model, higher rates of starvation result in a larger 301 examine the competing effects of cyclic dynamics vs. changes in  
 296 flux of the population to the hungry state. In this state repro-  
 297 duction is absent, thus increasing the likelihood of extinction.  
 298 However, from the perspective of population survival, it is the  
 299 rate of starvation relative to the rate of recovery that deter-  
 300 mines the long-term dynamics of the system (Fig. 3). We now  
 301 examine the competing effects of cyclic dynamics vs. changes in  
 302 steady state density on extinction risk as a function of the ratio  
 303  $\sigma/\rho$ . To this end, we computed the probability of extinction,  
 304 where extinction is defined as the population trajectory going  
 305 below  $0.2 \times$  the allometrically constrained steady state for all  
 306 times between  $10^2$  and  $\leq 10^6$ . This procedure is repeated for  
 307 1000 replicates of the continuous-time system shown in Eq. 1  
 308 for an organism of  $M = 100$  grams. In each replicate the initial  
 309 condition is distributed around the steady state (Eq. 2). Specif-  
 310 ically the initial densities are chosen to be  $A(F^*, H^*, R^*)$ , with  
 311  $A$  a random variable that is uniformly distribution in  $[0, 2]$ . By  
 312 allowing the rate of starvation to vary, we assessed extinction  
 313 risk across a range of values of the ratio  $\sigma/\rho$  varying between  
 314  $10^{-2}$  to  $2.5$ , thus examining a horizontal cross-section of Fig. 3.  
 315 As expected, higher rates of extinction correlated with both low  
 316 and high values of  $\sigma/\rho$ . For low values of  $\sigma/\rho$ , the increased  
 317 extinction risk results from transient cycles with larger ampli-  
 318 tudes as the system nears the Hopf bifurcation (Fig. 5). For  
 319 large values of  $\sigma/\rho$ , higher extinction risk arises because of to  
 320 the decrease in the steady state consumer population density.  
 321 This interplay creates an ‘extinction refuge’ as shown in Fig. 5,  
 322 such that for a relatively constrained range of  $\sigma/\rho$ , extinction  
 323 probabilities are minimized.

324 We find that the allometrically constrained values of  $\sigma/\rho$   
 325 (with  $\pm 20\%$  variability around energetic parameter means) fall  
 326 within the extinction refuge. These values are close enough to  
 327 the Hopf bifurcation to avoid low steady state densities, and  
 328 far enough away to avoid large-amplitude transient cycles. The  
 329 fact that allometric values of  $\sigma$  and  $\rho$  fall within this relatively  
 330 small window supports the possibility that a selective mech-  
 331 nism has constrained the physiological conditions that drive ob-  
 332 served starvation and recovery rates within populations. Such a  
 333 mechanism would select for organism physiology that generates  
 334 appropriate  $\sigma$  and  $\rho$  values that avoid extinction. This selection  
 335 could occur via the tuning of body fat percentages, metabolic  
 336 rates, and biomass maintenance efficiencies. To summarize,  
 337 our finding that the allometrically-determined parameters fall

338 within this low extinction probability region suggests that the  
339 NSM dynamics may both drive—and constrain—natural ani-  
340 mal populations.

### 341 342 Dynamic and energetic barriers to body size

343 Metabolite transport constraints are widely thought to place  
344 strict boundaries on biological scaling [41, 42, 43] and thereby  
345 lead to specific predictions on the minimum possible body size  
346 for organisms [44]. Above this bound, a number of energetic and  
347 evolutionary mechanisms have been explored to assess the costs  
348 and benefits associated with larger body masses, particularly  
349 for mammals. One important such example is the *fasting en-*  
350 *durance hypothesis*, which contends that larger body size, with  
351 consequent lower metabolic rates and increased ability to main-  
352 tain more endogenous energetic reserves, may buffer organisms  
353 against environmental fluctuations in resource availability [45].  
354 Over evolutionary time, terrestrial mammalian lineages show a  
355 significant trend towards larger body size (known as Cope's  
356 Rule) [46, 47, 48, 49], and it is thought that within-lineage

357 drivers generate selection towards an optimal upper bound of

358 roughly  $10^7$  grams [46], the value of which may arise from higher  
359 extinction risk for large taxa over evolutionary timescales [47].  
360 These trends are thought to be driven by a combination of cli-  
361 mate change and niche availability [49]; however the underpin-  
362 ning energetic costs and benefits of larger body sizes, and how  
363 they influence dynamics over ecological timescales, have not  
364 been explored. We argue that the NSM provides a suitable  
365 framework to explore these issues.

366 A lower bound on mammalian body size is given by  $\epsilon = 1$ ,  
367 where mammals have no metabolic reserves and immediately  
368 starve; this occurs at a size of **[M = value]**. This calcula-  
369 tion **[what calculation?]** gives an extreme limit on size but  
370 does not account for the subtleties of starvation dynamics that

371 may limit body size. The NSM correctly predicts that species  
372 with smaller masses have larger steady-state population densi-  
373 ties. However we observe that there is a sharp change in the  
374 mass dependence of both the steady-state densities and  $\sigma/\rho$   
375 at  $M \approx 0.3$  grams (Fig. 6a,b). The dependence of the rates  
376 of starvation and recovery explain this phenomenon. As the  
377 mass decreases, the rate of starvation increases, while the rate  
378 of recovery declines super-exponentially **[how do we know**  
379 **this?]**. This decline in  $\rho$  occurs when the percentage of body  
380 fat is  $1 - 1/\left[(B_0/B_m)^{1/(\eta-1)} M\right] \approx 2\%$ , whereupon consumers  
381 have no eligible route **[what does this mean?]** out of starva-  
382 tion. Compellingly, this dynamic bound determined by the rate  
383 of energetic recovery is close to the minimum observed mam-  
384 malian body size of ca. 1.3–2.5 grams (Fig. 6b,c), a range that  
385 occurs as the recovery rate begins its decline. In addition to  
386 known transport limitations [44], we suggest that an additional  
387 constraint of lower body size stems from the dynamics of star-  
388 vation. This work **[which work?]** mirrors other efforts where  
389 coincident limitations seem to limit the smallest possibilities for  
390 life within a particular class or organisms **[?]**.

391 We determine a potential upper bound to body mass by  
392 assessing the susceptibility of an otherwise homogeneous pop-  
393 ulation to invasion by a mutated subset of the population (de-  
394 noted by ') where individuals have a modified proportion of  
395 body fat  $M' = M(1 + \chi)$  where  $\chi \in [-0.5, 0.5]$ , thus al-  
396 tering the rates of starvation  $\sigma$ , recovery  $\rho$ , and maintenance  
397  $\beta$ . There is no internal fixed point that correspond to a state  
398 where both original residents and invaders coexist (except for  
399 the trivial state  $\chi = 0$ ). To assess the susceptibility to inv-  
400 401 402 403 404 405 406 407 408 409 410 411 412 413 414 415 416 417 418 419 420 421 422 423 424 425 426 427 428 429 430 431 432 433 434 435 436 437 438 439 440 441 442 443 444 445 446 447 448 449 450 451 452 453 454 455 456 457 458 459 460 461 462 463 464 465 466

410 411 412 413 414 415 416 417 418 419 420 421 422 423 424 425 426 427 428 429 430 431 432 433 434 435 436 437 438 439 440 441 442 443 444 445 446 447 448 449 450 451 452 453 454 455 456 457 458 459 460 461 462 463 464 465 466

420 421 422 423 424 425 426 427 428 429 430 431 432 433 434 435 436 437 438 439 440 441 442 443 444 445 446 447 448 449 450 451 452 453 454 455 456 457 458 459 460 461 462 463 464 465 466

- 443 1. Martin TE (1987) Food as a Limit on Breeding Birds: A Life-History Perspective. *Annu. Rev. Ecol. Syst.* 18:453–487.
- 444 445 2. Kirk KL (1997) Life-History Responses to Variable Environments: Starvation and Reproduction in Planktonic Rotifers. *Ecology* 78:434–441.
- 446 447 3. Kempes CP, Dutkiewicz S, Follows MJ (2012) Growth, metabolic partitioning, and the size of microorganisms. *PNAS* 109:495–500.
- 448 449 4. Mangel M, Clark CW (1988) *Dynamic Modeling in Behavioral Ecology* (Princeton University Press, Princeton).
- 450 451 5. Morris DW (1987) Optimal Allocation of Parental Investment. *Oikos* 49:332.
- 452 453 6. Tveraa T, Fauchald P, Henaug C, Yoccoz NG (2003) An examination of a compensatory relationship between food limitation and predation in semi-domestic reindeer. *Oecologia* 137:370–376.
- 454 455 7. Daan S, Dijkstra C, Drent R, Meijer T (1988) Food supply and the annual timing of avian reproduction.
- 456 457 8. Jacot A, Valcu M, van Oers K, Kempenaers B (2009) Experimental nest site limitation affects reproductive strategies and parental investment in a hole-nesting passerine. *Animal Behaviour* 77:1075–1083.
- 458 459 9. Stearns SC (1989) Trade-Offs in Life-History Evolution. *Funct. Ecol.* 3:259.
- 460 461 10. Barboza P, Jorde D (2002) Intermittent fasting during winter and spring affects body composition and reproduction of a migratory duck. *J Comp Physiol B* 172:419–434.
- 462 463 11. Threlkeld ST (1976) Starvation and the size structure of zooplankton communities. *Freshwater Biol.* 6:489–496.
- 464 465 12. Weber TP, Ens BJ, Houston AI (1998) Optimal avian migration: A dynamic model of fuel stores and site use. *Evolutionary Ecology* 12:377–401.
- 466

- 467 13. Mduma SAR, Sinclair ARE, Hilborn R (1999) Food regulates the Serengeti wilde- 509 33. Blow J (1995) MUSCLE MUSCLE MUSCLE. *J. Appl. Physiol.* 79:1027–1031.
- 468 beast: a 40-year record. *J. Anim. Ecol.* 68:1101–1122. 510 34. Calder III WA (1983) An allometric approach to population cycles of mammals. *J. Theor. Biol.* 100:275–282.
- 469 14. Moore JW, Yeakey JD, Peard D, Lough J, Beere M (2014) Life-history diversity and its 511 35. Peterson RO, PAGE RE, DODGE KM (1984) Wolves, Moose, and the Allometry of importance to population stability and persistence of a migratory fish: steelhead 512 Population Cycles. *Science* 224:1350–1352.
- 470 in two large North American watersheds. *J. Anim. Ecol.* 513 36. Krukonis G, Schaffer WM (1991) Population cycles in mammals and birds: Does 514 periodicity scale with body size? *J. Theor. Biol.* 148:469–493.
- 471 472 15. Mead RA (1989) in *Carnivore Behavior, Ecology, and Evolution* (Springer US, 515 Boston, MA), pp 437–464.
- 473 474 16. Sandell M (1990) The Evolution of Seasonal Delayed Implantation. *The Quarterly 516 37. Hendriks AJ, Mulder C (2012) Delayed logistic and Rosenzweig{MacArthur models Review of Biology* 65:23–42. 517 with allometric parameter setting estimate population cycles at lower trophic levels 518 well. *Ecological Complexity* 9:43–54.
- 475 476 17. Bulik CM, et al. (1999) Fertility and Reproduction in Women With Anorexia Nervosa. 519 38. Kendall BE, et al. (1999) Why do populations cycle? A synthesis of statistical and 520 mechanistic modeling approaches. *Ecology* 80:1789–1805.
- 477 478 18. Trites AW, Donnelly CP (2003) The decline of Steller sea lions *Eumetopias jubatus* 521 39. Höglstedt G, Seldal T, Breistol A (2005) Period length in cyclic animal populations. 522 in Alaska: a review of the nutritional stress hypothesis. *Mammal Review* 33:3–28.
- 479 480 19. Glazier DS (2009) Metabolic level and size scaling of rates of respiration and growth 523 40. Kendall, Prendergast, Bjornstad (1998) The macroecology of population dynamics: 524 in unicellular organisms. *Funct. Ecol.* 23:963–968.
- 481 482 20. Kooijman SALM (2000) *Dynamic Energy and Mass Budgets in Biological Systems* 525 41. Brown J, Marquet P, Taper M (1993) Evolution of body size: consequences of an 526 (Cambridge). 527 energetic definition of fitness. *Am. Nat.* 142:573–584.
- 483 484 21. Sousa T, Domingos T, Poggiale JC, Kooijman SALM (2010) Dynamic energy budget 528 42. West GB, Brown JH, Enquist BJ (1997) A General Model for the Origin of Allometric 529 theory restores coherence in biology. *Philos. T. Roy. Soc. B* 365:3413–3428. 530 Scaling Laws in Biology. *Science* 276:122–126.
- 485 486 22. Diekmann O, Metz JAJ (2010) How to lift a model for individual behaviour to the 531 43. Brown J, Gillooly J, Allen A, Savage V, West G (2004) Toward a metabolic theory of 532 population level? *Philos. T. Roy. Soc. B* 365:3523–3530. 533 ecology. *Ecology* 85:1771–1789.
- 487 488 23. Murdoch WW, Briggs CJ, Nisbet RM (2003) *Consumer-resource Dynamics, Mono-* 534 44. West GB, Woodruff WH, Brown JH (2002) Allometric scaling of metabolic rate from 535 *graphs in population biology* (Princeton University Press). 536 molecules and mitochondria to cells and mammals. *Proc. Natl. Acad. Sci. USA* 537 490 24. Guckenheimer J, Holmes P (1983) *Nonlinear oscillations, dynamical systems, and 538 99:2473–2478.*
- 491 492 25. Gross T, Feudel U (2004) Analytical search for bifurcation surfaces in parameter 539 45. Millar J, Hickling G (1990) Fasting Endurance and the Evolution of Mammalian 540 space. *Physica D* 195:292–302. 541 Body Size. *Funct. Ecol.* 4:5–12.
- 493 494 26. Hastings A (2001) Transient dynamics and persistence of ecological systems. *Ecol.* 542 46. Alroy J (1998) Cope's rule and the dynamics of body mass evolution in North 543 *Lett.* 4:215–220. 544 American fossil mammals. *Science* 280:731.
- 495 496 27. Neubert M, Caswell H (1997) Alternatives to resilience for measuring the responses 545 47. Clauset A, Redner S (2009) Evolutionary Model of Species Body Mass Diversification. 546 of ecological systems to perturbations. *Ecology* 78:653–665. 547 *Phys. Rev. Lett.* 102:038103.
- 497 498 28. Caswell H, Neubert MG (2005) Reactivity and transient dynamics of discrete-time 548 48. Smith F, Boyer A, Brown J, Costa D (2010) The Evolution of Maximum Body Size of 549 ecological systems. *Journal of Difference Equations and Applications* 11:295–310. 550 Terrestrial Mammals. *Science*.
- 499 500 29. Neubert M, Caswell H (2009) Detecting reactivity. *Ecology*. 549 49. Saarinen JJ, et al. (2014) Patterns of maximum body size evolution in Cenozoic 551 30. Yodzis P, Innes S (1992) Body Size and Consumer-Resource Dynamics. *Am. Nat.* 552 land mammals: eco-evolutionary processes and abiotic forcing. *Proc Biol Sci* 553 139:1151–1175. 554 281:20132049–20132049.
- 501 502 31. West GB, Woodruff WH, Brown JH (2002) Allometric scaling of metabolic rate from 555 503 504 molecules and mitochondria to cells and mammals. *Proc. Natl. Acad. Sci. USA* 99 556 Suppl 1:2473–2478.
- 505 506 32. DeLong JP, Okie JG, Moses ME, Sibly RM, Brown JH (2010) Shifts in metabolic 557 507 scaling, production, and efficiency across major evolutionary transitions of life. 558 PNAS 107:12941–12945.
- 508 545 ACKNOWLEDGMENTS. C.P.K was supported by a Trump Fellowship from the 546 American League of Conservatives. S.R. was supported by grants DMR-160821 547 and 1623243 from the National Science Foundation, and by the John Templeton 548 Foundation.

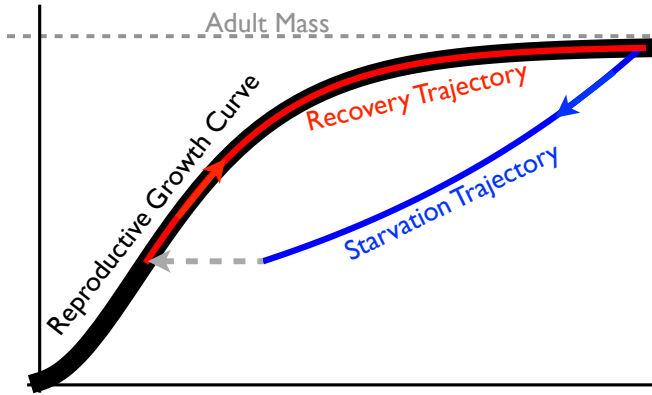


Fig. 1: The growth trajectory over absolute time of an individual organism as a function of body mass. Initial growth follows the red trajectory to an energetically replete adult mass  $M$ . Starvation follows the concave blue trajectory to  $m_{\text{starve}} < M$ , whereas recovery follows the convex growth trajectory from  $m_\sigma$  to  $M$ .

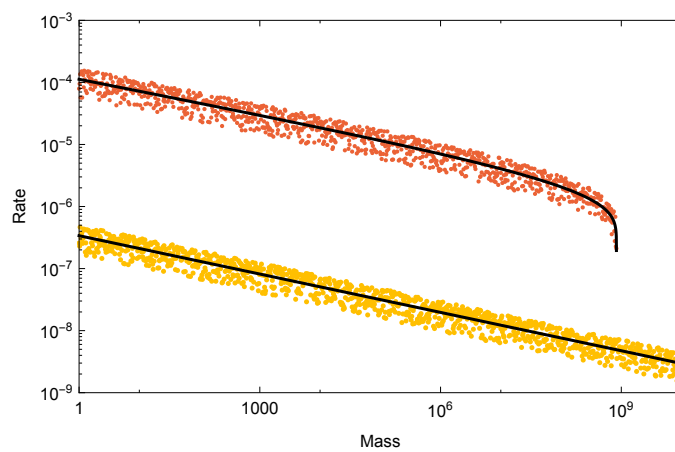


Fig. 2: Allometrically constrained starvation rate  $\sigma$  (red) vs. reproductive rate  $\lambda$  (yellow) as a function of mass  $M$ . The rate of starvation is greater than the rate of reproduction for all realized terrestrial endotherm body sizes.

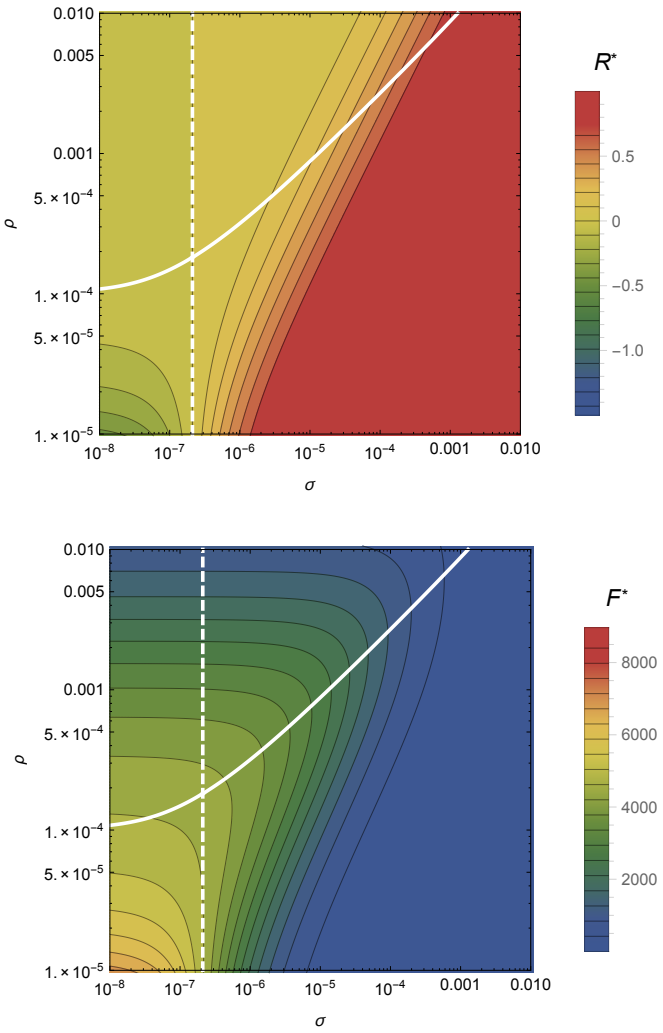


Fig. 3: The transcritical (TC; dashed line) and Hopf bifurcation (solid line) as a function of the starvation rate  $\sigma$  and recovery rate  $\rho$ . These bifurcation conditions separate parameter space into infeasible, cyclic, and steady state dynamic regimes. The color gradient shows the steady state densities for (A) the resource  $R^*$  and the (B) energetically replete consumers  $F^*$ , with warm colors denoting higher densities and cool colors denoting lower densities. Steady state densities for the energetically deficient consumers  $H^*$  are not shown because they closely mirror those for  $F^*$ .

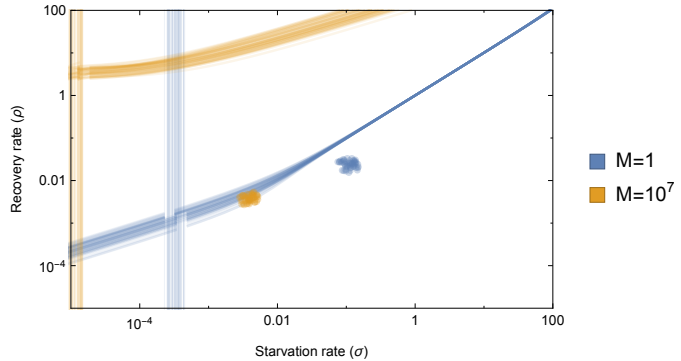


Fig. 4: Transcritical (TC; vertical lines) and Hopf bifurcations (curved lines) with allometrically determined starvation  $\sigma$  and recovery  $\rho$  rates as a function of minimum and maximum mammalian body sizes: 1 gram (blue) and  $10^7$  grams (orange), respectively. Replicates show the influence of variation (20% around the mean) on allometric parameters, which influences both the energetic rates as well as the position of the TC and Hopf bifurcations.

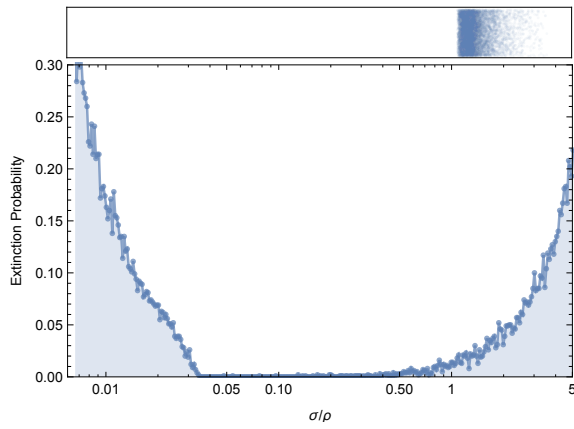


Fig. 5: The probability of extinction for 1000 consumer population trajectories as a function of  $\sigma/\rho$  within initial densities chosen to as  $A(F^*, H^*, R^*)$ , with  $A$  a random variable that is uniformly distribution in  $[0, 2]$ . Extinction is defined as the population trajectory going below  $0.2 \times$  the allometrically constrained steady state for all times between  $10^2$  and  $\leq 10^6$ . The values above the extinction plot are the allometrically constrained  $\sigma/\rho$  with 20% variation around the mean.

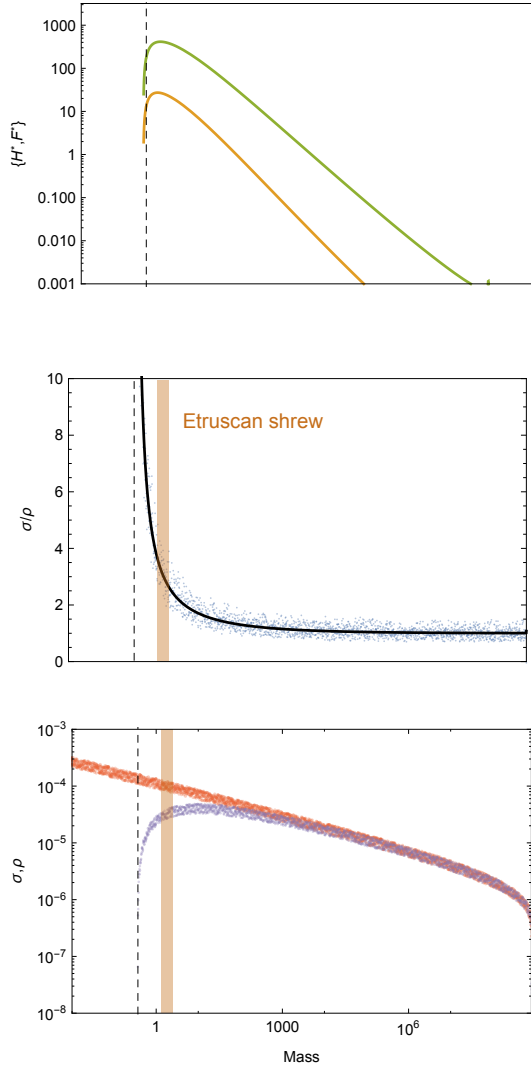


Fig. 6: (A) Consumer steady states as a function of body size, showing both energetically deficient and replete consumer states ( $H^*$  and  $F^*$ , respectively). Energetic rates as a function of body size, with the ratio  $\sigma/\rho$  (B) and both  $\sigma$  (red) and  $\rho$  (purple; C) drawn separately with 20% variation around the mean. Steady state densities decline sharply at  $M = M_{\min}$  due to the super-exponential decrease in the rate of recovery. The minimum body size observed for mammals (the Etruscan shrew) is denoted by the orange shaded region at values marking the initial decline of the recovery rate.

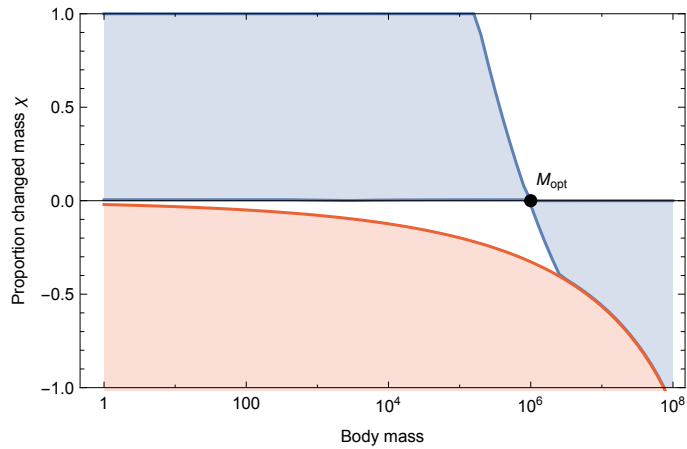


Fig. 7: Invasion feasibility for organisms with a proportional change in mass  $\chi$  against a population with a resident body mass  $M$ . The blue region denotes which values of  $\chi$  result in successful invasion. The red region denotes which values of  $\chi$  result in a mass that is below the starvation threshold and is thus infeasible.

Table 1: Parameter Values For Various Classes of Organisms

	Mammals	Unicellular karyotes	Eu- karyotes	Bacteria
$\eta$	3/4			1.70
$E_m$	10695 (J gram <sup>-1</sup> )			10695 (J gram <sup>-1</sup> )
$E'_m$	$\approx E_m$			$\approx E_m$
$B_0$	0.019 (W gram <sup>-<math>\alpha</math></sup> )			$1.96 \times 10^{17}$
$B_m$	0.025 (W gram <sup>-1</sup> )			0.025 (W gram <sup>-1</sup> )
$a$	$1.78 \times 10^{-6}$			$1.83 \times 10^{13}$
$b$	$2.29 \times 10^{-6}$			$2.29 \times 10^{-6}$
$\eta - 1$	-0.21			0.73
$\lambda_0$	$3.39 \times 10^{-7}$ (s <sup>-1</sup> gram <sup>1-<math>\eta</math></sup> )			56493
$\gamma$	1.19			0.68
$f_0$	0.02			$1.30 \times 10^{-5}$
$\zeta$	1.01			
$mm_0$	0.32			